CGMS-XXXIII JMA-WP-11
Prepared by JMA
Agenda Item: II/2
Discussed in WG II

Preliminary Validation Report on MTSAT-1R Imagery Data

This paper reports on preliminary validation on MTSAT-1R imagery data.

Preliminary Validation Report on MTSAT-1R Imagery Data

1. Introduction

MTSAT-1R was launched on 26 February 2005, and its meteorological mission started operating at 03 UTC 28 June 2005. JAMI, the new imager aboard MTSAT-1R, provides more frequent earth images with higher spatial and quantization resolutions than VISSR aboard GMS-5. In addition to these refinements, the new channel over the shortwave infrared window band is installed to provide more cloud information.

GOES-9 of NOAA/NESDIS was operated to serve as a back up satellite. Even after the starting of the MTSAT-1R meteorological operation, GOES-9 has been continuously catching earth images, which allowed validating MTSAT-1R images. This report reviews the calibration and navigation status of MTSAT-1R HRIT images, by comparing them with GOES-9 simultaneous observations.

2. Specification of MTSAT-1R imagery data

Table 1 shows comparison of specification associated with raw images observed by MTSAT-1R, GOES-9 and GMS-5. The geosynchronous position of MTSAT-1R is at 140 E, which is the same as GMS-5. GOES-9's position is at 155 E. The spatial resolutions of MTSAT-1R are higher than those of GMS-5 for all channels. The quantization resolution of MTSAT-1R is 1024, which is also higher than that of GMS-5. Accordingly, the accuracy of radiance observed by MTSAT-1R is better than that by GMS-5. MTSAT-1R observes northern hemisphere half-disk images 24 times a day and southern hemisphere half-disk images 8 times a day, in addition to hourly full-disk images.

Figure 1 shows the spectral response functions (SRFs). The observing bands of MTSAT-1R/JAMI IR1 and IR2 lie on the infrared window region where water vapor continuum and aerosol are the major source of absorption. Compared to GMS-5/VISSR, MTSAT-1R IR1 and IR2 are separated with each other, whereas the IR2 band of GMS-5 overlaps with that of IR1. MTSAT-1R IR3 channel lies on more water vapor absorbing region than GMS-5 IR3. MTSAT-1R IR4, new channel similar to that of GOES-9, observes images over the region of the shortwave infrared window. This channel is expected to provide cloud information in addition to IR1 and IR2, particularly low-level cloud images at nighttime.

The central wavelengths and wavenumbers of MTSAT-1R infrared channels as well as Planck band correction coefficients are shown in Appendix. The central wavelengths of IR1, IR2, IR3 and IR4 computed based upon SRFs are 10.8, 12.0, 6.8 and 3.8 μm,

respectively.

Table 1 Comparison of specification

Satellite	MTSAT-1R		GOES-9		GMS-5	
Imager	JAMI		Imager		VISSR	
Operation (West Pacific)	28 Jun. 2005 to present		22 May 2004 to present		13 Jun. 1995 to 22 May 2004	
Geo. position	140 E		155 E		140 E	
Raw Data Format	HRIT		GVAR		VISSR	
Number of channels	5		5		4	
Band	Wavelength (μm)	Accuracy	Wavelength (μm)	Accuracy	Wavelength (μm)	Accuracy
VIS (Visible)	0.55 – 0.90	6.5SNR@2.5%	0.55 – 0.75	(NA)	0.55 – 0.9	6.5SNR@2.5%
IR1 (IR window 1)	10.3 – 11.3	0.18@300K	10.2 – 11.2	0.11@300K	10.5 – 11.5	0.35@300K
IR2 (IR window 2)	11.5 – 12.5	0.18@300K	11.5 – 12.5	0.14@300K	11.5 – 12.5	0.35@300K
IR3 (WV)	6.5 – 7.0	0.15@300K	6.5 – 7.0	0.09@300K	6.5 – 7.0	0.22@300K
IR4 (SWIR)	3.5 – 4.0	0.18@300K	3.8 – 4.0	(NA)		
Spatial resolution at nadir	VIS: 1 km IR1–4: 4 km		VIS: 1 km IR1, 2, 4: 4 km IR3: 8 km		VIS: 1.25 km IR1–3: 5 km	
Num. of quantization levels	VIS: 1024 IR: 1024		VIS: 1024 IR: 1024		VIS: 64 IR: 256	
Observing frequency (times/day)	Full disk: 24 Half disk: 24 (N.H.) 8 (S.H.)		Full disk: 24 (hourly) 4 (wind) Half disk: 13		Full disk: 24 (hourly) 4 (wind)	

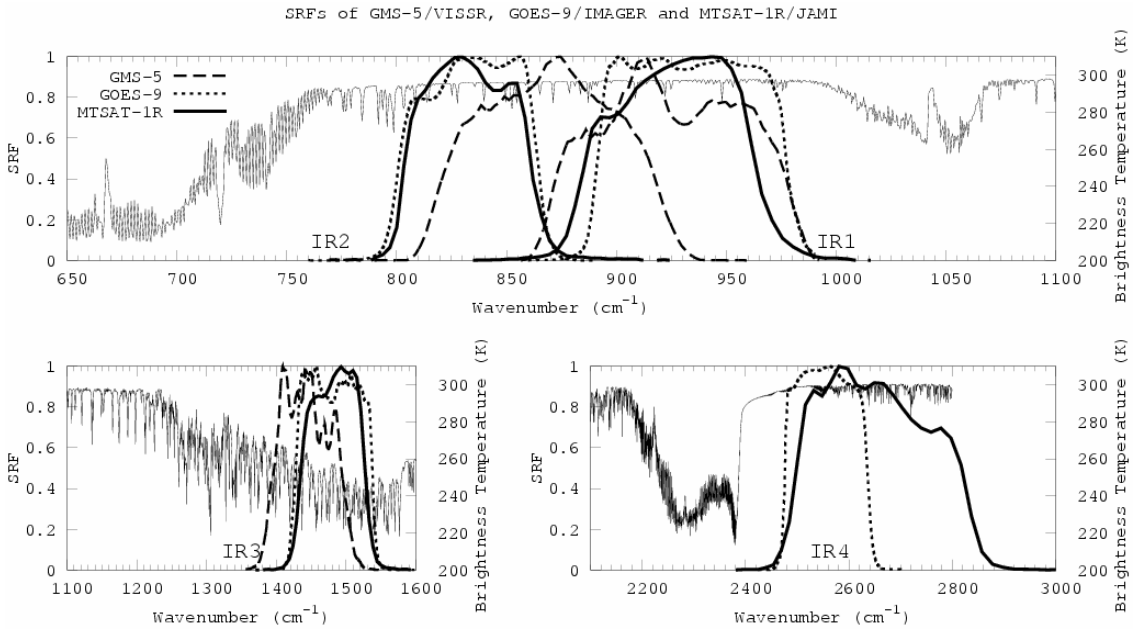

Figure 1 Spectral response functions (SRFs) of infrared channels of MTSAT-1R/JAMI (solid line), GOES-9/Imager (dotted line) and GMS-5/VISSR (broken line). The thin lines represent the brightness temperatures of out-going radiances from top of the atmosphere computed by LBLRTM (AGR) assuming the U.S. standard atmosphere.

3. Validation of image location

To survey the image location accuracy statistically, landmark matching is diagnosed. To evaluate the accuracy of the most recent available IR1 images, those observed from 14 to 18 October are analyzed. The image-matching algorithm is originally constructed based upon the cloud tracking technique used to retrieve AMVs. The result indicates that the total errors are around 0.7 pixels in horizontal and 0.6 to 0.9 pixels in vertical by standard deviation. Since further tune-up is underway, the accuracy of image location is expected to be improved shortly.

4. Validation of infrared channel calibration

The MTSAT-1R/JAMI infrared channels are dynamically calibrated in real-time by onboard system measuring a warm black body and cold space. SRFs measured in laboratory before launch are used to compute brightness temperatures and radiances from digital count values. This section reviews the MTSAT-1R infrared calibration by comparing its images to ones observed by GOES-9 simultaneously. Two types of comparison are conducted, a limited-condition comparison and all-condition comparison.

The limited-condition comparison uses brightness temperatures observed at cloud free area over the ocean only. The comparing method is the same as the one used in the report on intercalibration between GMS-5 and GOES-9 infrared channels (Tahara et al, 2004). To match up observations by the two satellites, brightness temperatures are averaged within 0.25 latitude and longitude degree boxes. In the comparison, the boxes of entirely cloud free area over the ocean are selected. To detect cloud, an algorithm reported by Yasuda and Shirakawa (1999) is used. The compared region ranges from 60 N to 60 S and from 145 E to 150 E to mitigate the difference of radiative paths from an observed point to the two satellites. Six-hourly images at 00, 06, 12 and 18 UTC are compared. The sampling period is from 1 July to 31 August 2005.

The all-condition comparison evaluates brightness temperatures observed under both clear and cloudy conditions over both land and ocean. The object of this comparison is to review both high and low temperature region. The compared domain is limited within the region from 60 N to 60 S and from 147 E to 148 E to make radiative path difference small. Since this comparison is performed pixel by pixel, its result includes not only radiative characteristic difference but also image navigation error. The sampling period is from 12 to 29 August 2005.

4.1 *IR1 (10.8 μm)*

Figure 2(a) shows the limited-condition comparison of the window channel IR1.

The comparison shows the differences are small as expected by MODTRAN simulation. The mean difference, MTSAT-1R minus GOES-9, is –0.42 K, and the standard deviation is 0.32 K.

Figure 2(b) shows the all-condition comparison of IR1. It shows that the MTSAT-1R temperatures are well correlated to the GOES-9 temperatures as seen in the limited-condition comparison. The mean difference is –0.75 K. Viewing the region of temperature lower than 260 K, where no sample is obtained in the limited-condition comparison, particular difference cannot be seen. The histogram of temperature differences between MTSAT-1R and GOES-9 (the figure not shown) follows the Gaussian distribution. As a consequence, no substantial calibration error is recognized in association with MTSAT-1R IR1.

4.2 *IR2 (12.0 μm)*

As IR1, no systematic calibration error is recognized. The mean difference is nearly neutral, +0.42 K by the limited-condition comparison and +0.09 K by the all-condition comparison. The standard deviation of clear-sky observed temperature differences between the two satellites is small, 0.38 K.

4.3 *IR3 (6.8 μm)*

Figure 3(a) and (b) show the limited-condition comparison and the all-condition comparison respectively regarding the water vapor channel, IR3. The results show that the temperatures are well correlated between MTSAT-1R and GOES-9. In terms of mean differences, it is nearly neutral in total, +0.34 K by the limited-condition comparison and –0.62 K by all-condition comparison, respectively. The standard deviations are 0.64 K by the limited-condition comparison and 2.01 K by all-condition comparison. No substantial calibration error can be recognized.

4.4 *IR4 (3.8 μm)*

The calibration process regarding MTSAT-1R IR4 is currently under review. The comparison of IR4 nighttime images against GOES-9 shows that the mean differences in the limited-condition and the all-condition comparison are currently –9.06 K and –8.69 K, respectively. The modification of the calibration process is in progress.

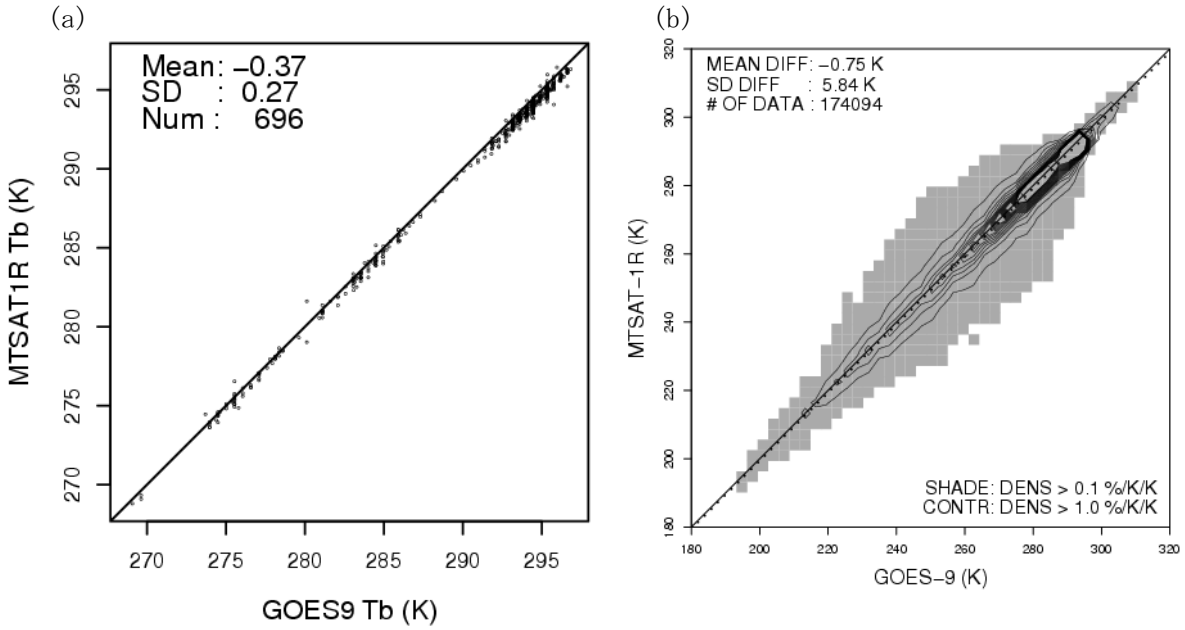

Figure 2 Comparisons of IR1 brightness temperatures between MTSAT-1R observations and GOES-9 observations at (a) cloud free area over the ocean within the region from 60 N to 60 S and from 145 E to 150 E and (b) all data within the region from 60 N to 60 S and from 147 E to 148 E. The mean difference and standard deviation between a vertical element and a horizontal element are shown along with the number of samples. The statistical period is (a) from 1 July to 31 August 2005 and (b) from 12 to 21 August 2005.

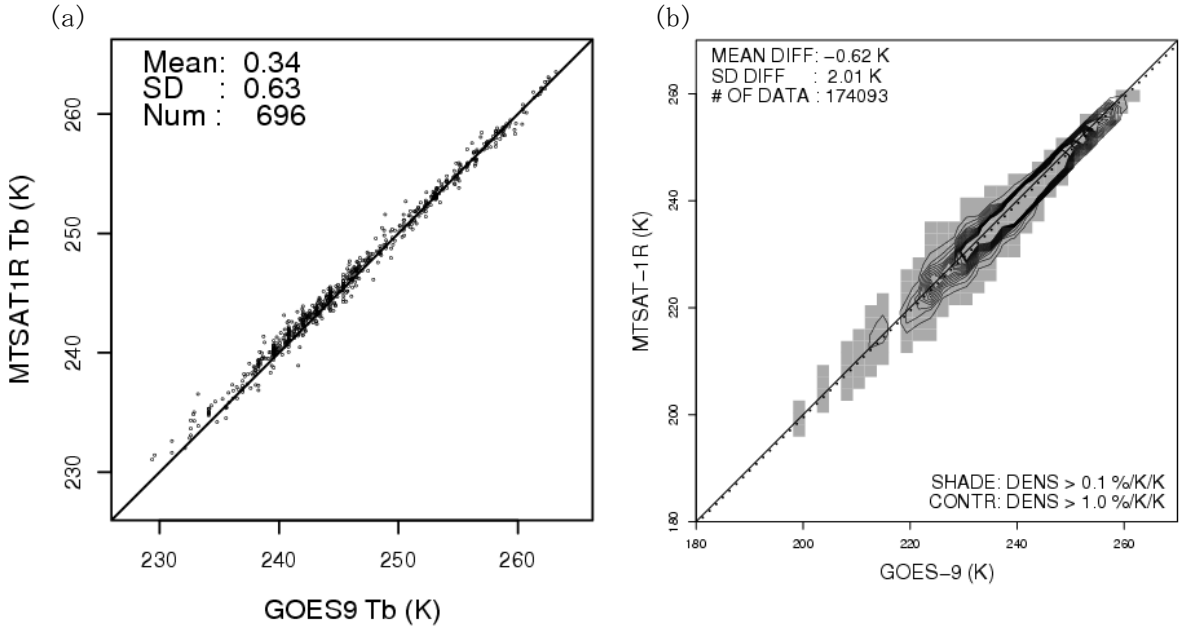

Figure 3 The same as Figure 2, but IR3 comparisons.

5. Validation of visible channel calibration

This section reviews the status of MTSAT-1R visible channel images. It is observed that the amplitude of electrical signal coming out of the MTSAT-1R/JAMI visible channel has fell to half of the value at the pre-launch test, which has no adverse effect on the conventional use by relevant organs. Hence, the calibration parameters of the visible channel were adjusted based on intercalibration with NOAA-16/AVHRR channel 1 before the commencement of MTSAT-1R operation. No dynamic calibration for the visible channel is performed for the operation.

Figure 4 shows the time series of the largest albedo values at the 99.9th, 98.0th, 90.0th, 70.0th and 40.0th percentile in all the pixels of visible data observed at 06 UTC. The target period is from 30 June to 16 October 2005. The sensitivity trend of the visible channel can be monitored by this histogram (Tokuno et al, 2001). Figure 4(a) shows the trend of MTSAT-1R and Figure 4(b) shows that of GOES-9.

Until the end of August, the trend of albedos at the 70.0th percentile in Figure 4(a) resides around 0.11 with small variation. It indicates that 70 % of albedos stably ranged from 0 to 0.11, and that no systematical change is observed in that albedo range. However, albedos at the 99.9th percentile show a decreasing trend until August. While 99.9 % of albedos ranges from 0 to 0.81 on 30 June, it ranges from 0 to 0.67 on 31 August. The decreasing trend is seen in the albedos at the 98.0th and 90.0th percentile as well. Meanwhile, such decreasing trend is not seen in the GOES-9 albedos shown in Figure Figure 4(b). Hence, the trend seen until August in Figure Figure 4(a) is not supposed to be caused by seasonal or other natural reason.

The albedo trends of MTSAT-1R and GOES-9 have been consistent with each other since September. The decreasing trend isn't seen in albedos at the 99.9th percentile in both Figure Figure 4(a) and (b). The trends of MTSAT-1R and GOES-9 albedos at the 98.0th and 90.0th percentile are decreasing mutually. Slight decreasing trend is seen in albedos at the 70.0th percentile of both MTSAT-1R and GOES-9.

It is possible that the MTSAT-1R visible channel might have undergone a slow transient change in its property until August. Since the study uses images observed only during initial three and a half months, further monitoring is needed to validate the property of the visible channel.

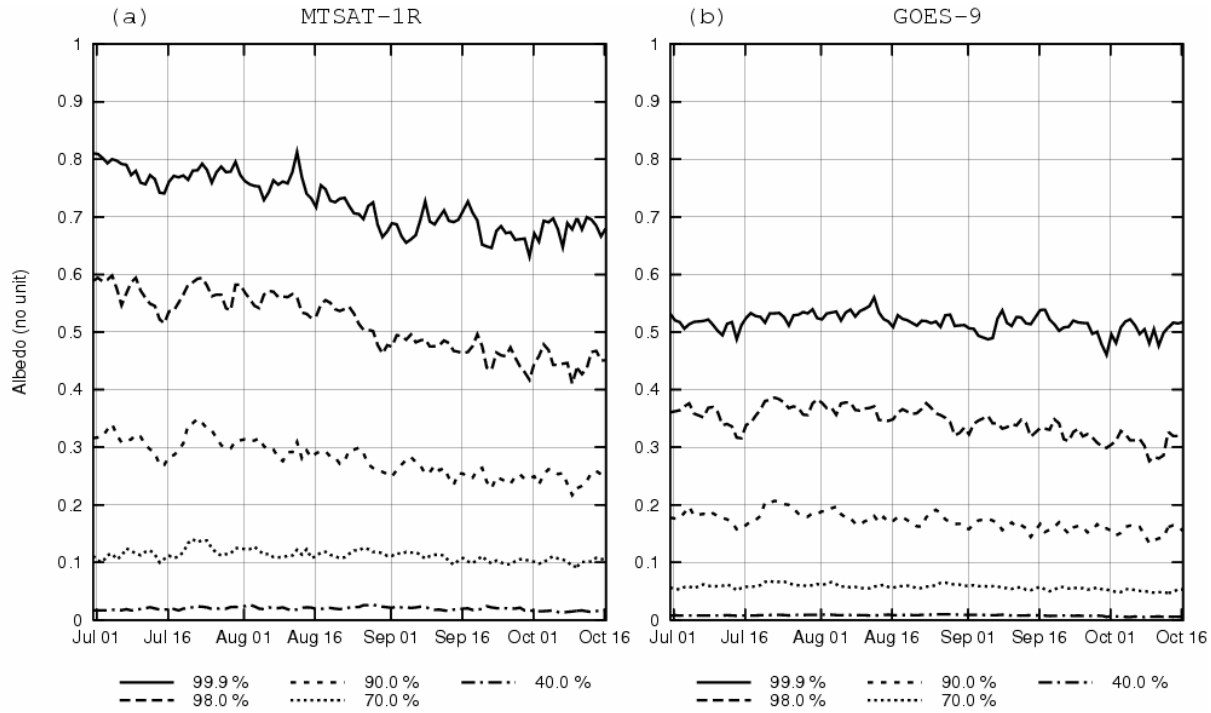

Figure 4 Figure shows the time series of the largest albedo values in the 99.9th, 98.0th, 90.0th, 70.0th, 40.0th percentile in all the pixels of visible data observed at 06 UTC; (a) MTSAT-1R/JAMI and (b) GOES-9/VISSR. The target period is from 30 June to 16 October 2005.

6. Conclusion

MTSAT-1R navigation and calibration status has been studied by reviewing three and a half months operational HRIT imagery data from 28 June 2005. The accuracy of HRIT image location has been diagnosed by landmark matching evaluation. The latest evaluation shows that the image location error is within a pixel by standard deviation. To review the calibration status of the MTSAT-1R infrared channels, the observed images have been compared to GOES-9 simultaneous observations. The result shows that MTSAT-1R IR1, IR2, and IR3 are well calibrated and no particular systematic error is found. The brightness temperature of MTSAT-1R IR4 is lower than that of GOES-9 IR4. The calibration process of MTSAT-1R IR4 is currently under review. The calibration of the MTSAT-1R visible channel has been also studied. It is possible that the trend monitor of the MTSAT-1R visible channel may indicate a sign of a slow transient change in the range of albedo larger than 0.11 until August 2005. From September, the trend of MTSAT-1R corresponds to that of GOES-9, and no clear change is recognized.

Appendix: Central wavelength/wavenumber and Planck band correction coefficients

To convert a brightness temperature into a radiance, it is convenient to compute in advance a central wavelength or wavenumber of the band and the band correction coefficients of the Planck function from a spectral response function. In this section, derivations of these parameters are presented.

Table 2 shows the central wavelength of the MTSAT-1R infrared channels computed by

$$\nu_i = \frac{\int \nu S_i(\nu) d\nu}{\int S_i(\nu) d\nu},$$

where i, ν and $S_i(\nu)$ denotes a channel number, a wavelength or wavenumber and the spectral response function of the channel i, respectively. Using the central frequency and band correction coefficients C_1, C_2 and C_3 shown in Table 3, the radiance I_i and the brightness temperature T are convertible by

$$I_i \approx B(\nu_i, T_e), \qquad T_e = C_1 + C_2 T + C_3 T^2,$$

where B represents the monochromatic Planck function and T_e is a virtual value called an effective temperature.

Table 2 Central wavelength/wavenumber of MTSAT-1R/JAMI infrared channels

	IR1	IR2	IR3	IR4
Wavelength (μm)	10.81542	12.01964	6.75458	3.78478
Wavenumber (cm^{-1})	926.622	833.169	1482.218	2653.004

Table 3 Band correction coefficients of the Planck function. T_e denotes an effective temperature. The accuracy of conversion from a radiance to a brightness temperature is within 0.05 K by a linear approximation and 0.005 K by a quadratic approximation.

Ch.		Wavelength Space			Wavenumber Space		
		C_1	C_2	C_3	C_1	C_2	C_3
IR1	$T_e = C_1 + C_2 T$	-5.40390E-02	9.99913E-01		3.55264E-01	9.98777E-01	
	$T_e = C_1 + C_2 T + C_3 T^2$	4.61522E-01	9.95816E-01	7.87838E-06	4.94015E-01	9.97674E-01	2.12028E-06
	$T = C_1 + C_2 T_e + C_3 T_e^2$	-4.61397E-01	1.00418E+00	-7.88043E-06	-4.95017E-01	1.00233E+00	-2.12808E-06
IR2	$T_e = C_1 + C_2 T$	-9.98901E-02	1.00023E+00		1.93829E-01	9.99266E-01	
	$T_e = C_1 + C_2 T + C_3 T^2$	2.60175E-01	9.97365E-01	5.50223E-06	2.91988E-01	9.98486E-01	1.49998E-06
	$T = C_1 + C_2 T_e + C_3 T_e^2$	-2.59858E-01	1.00263E+00	-5.49849E-06	-2.92356E-01	1.00152E+00	-1.50329E-06
IR3	$T_e = C_1 + C_2 T$	2.34635E-01	9.99093E-01		3.78131E-01	9.99123E-01	
	$T_e = C_1 + C_2 T + C_3 T^2$	4.18015E-01	9.97636E-01	2.80226E-06	4.19855E-01	9.98791E-01	6.37599E-07
	$T = C_1 + C_2 T_e + C_3 T_e^2$	-4.18745E-01	1.00237E+00	-2.80990E-06	-4.20350E-01	1.00121E+00	-6.39280E-07
IR4	$T_e = C_1 + C_2 T$	2.06947E+00	9.95116E-01		2.35676E+00	9.96955E-01	
	$T_e = C_1 + C_2 T + C_3 T^2$	2.23844E+00	9.93774E-01	2.58206E-06	2.24764E+00	9.97822E-01	-1.66754E-06
	$T = C_1 + C_2 T_e + C_3 T_e^2$	-2.25225E+00	1.00627E+00	-2.62025E-06	-2.25244E+00	1.00217E+00	1.68288E-06

Reference

(Printed documents)

Berk, A., L. S. Bernstein and D. C. Roberson, 1989: MODTRAN: A Moderate Resolution Model for LOWTRAN 7. GL-TR-89-0122.

Meteorological Satellite Center, 1997: The GMS User's Guide Third Edition.

Tahara, Y., N. Ohkawara and A. Okuyama: Intercalibration of the infrared Channels between GMS-5 and GOES-9, Meteorological Satellite Center Technical Note, No. 44, 1-18.

Tokuno, M., S. Kurihara, Y. Kaido, 2001: Operational GMS-5 VISSR Calibration, Meteorological Satellite Center Technical Note, No. 39, 13-32.

Yasuda, Hiroaki, and Yoshishige Shirakawa, 1999: Improvement of the Derivation Method of Sea Surface Temperature from GMS-5 Data. Meteorological Satellite Center Technical Note, No. 37, 19-33. (written in Japanese)

(Web sites on the Internet)

Atmospheric and Environmental Research Inc. (AER): Line-By-Line Radiative Transfer Model (LBLRTM),
http://rtweb.aer.com/

NOAA/NESDIS: Geostationary Operational Environmental Satellites.
http://www.oso.noaa.gov/goes/